The Simulation of Nearshore Wave Energy Converters and their Associated Impacts around the Outer Hebrides

Charles E. Greenwood[#1], David Christie[#2], Vengatesan Venugopal[*3]

[#]*Lews Castle College, University of the Highlands and Islands*
Stornoway, Isle of Lewis, Scotland

[1]charles.greenwood@uhi.ac.uk

[2]david.christie@uhi.ac.uk

[*]*University of Edinburgh*
School of Engineering, The University of Edinburgh, Edinburgh, Scotland

[3]v.venugopal@ed.ac.uk

***Abstract*— The results of a numerical wave modelling study carried out to assess the nearshore effects of wave energy extraction on the local wave climate by an array of hypothetical wave energy converters (WECs) are presented in this paper. This study uses the Danish Hydraulic Institute's (DHI) MIKE 21 Spectral Wave model to identify and test three different techniques of simulating hypothetical WECs on a regional scale. The results suggest the more complex approach of simulating absorption using directional and frequency absorption spectra in addition to the effects of wave reflections yields a more realistic simulation. This technique was further applied to a potential wave energy deployment site consisting of an array of 30 WEC devices identified by the Crown Estate in the Outer Hebrides in the United Kingdom. The boundary input used seasonal averaged data to represent winter, summer and a complete year's wave spectra. The results suggest there is an average shoreline reduction in wave power behind the array of 5% with a peak value of 9.5%. The inclusion of wave reflection in to the model leads to a larger average percentage change in wave power of 7.5% 300m from the devices. While the results of this study also provide an insight into the distribution of wave energy around a nearshore array, this study focuses on developing advanced technique for the simulation of WECs.**

***Keywords*— Wave Energy, Mike 21 Spectral Wave model, Wave farm, Wave modelling, Nearshore impacts.**

I. INTRODUCTION

As global energy demand increases renewable energy offers a clean solution to help mitigate anthropogenic climate change. In recent years alternative technologies have been explored with the intention of up scaling them to help provide a broad energy mix. As these technologies evolve, governmental support and legislation is being implemented to ensure the generation of clean energy. The Scottish government has led the way by setting a target of producing 100% of its electrical energy demand by 2020 from clean renewable sources [1]. However international legislation states that any large scale developments of this kind require an Environmental Impact Assessment (EIA). This assessment reviews the possible impacts a proposed development may have on the existing environment. This process has been applied to existing renewable energy projects highlighting the potential environmental implications of the installation, operational and decommissioning stages of a project [2, 3]. With ocean waves containing vast amounts of energy a niche was created for developing devices to withstand and extract this energy in a cost efficient manner. With the imminent transition from single Wave Energy Converter (WEC) deployments to large arrays, the potential environmental effects caused by alterations in the wave climate are unknown. As no large scale arrays have been deployed the quantification of the change in wave climate has been conducted using laboratory experiments and computational models.

The west coast of the Isle of Lewis (Outer Hebrides) has been highlighted as an area of high wave resource. This has lead to the interest of several device developers. Aquamarine Power have successfully gained two lease sites on Lewis with the potential of extracting up to 40MW [4], Pelamis Wave Power have acquired a lease allowing up to 10MW development [5] and Voith Hydro Wavegen were granted a lease to construct a 30MW breakwater. However the development proposed by Voith Hydro Wavegen has been suspended [6]. This would have allowed the cumulative extraction of up to 80MW along the north-west coast of Lewis. The original planned development areas can be seen in Fig. 1. The large existing resource provides a lucrative opportunity for any successful device developer. With the interest of several developers, the spatial distribution of the resources and the resultant wave-device interactions require an in-depth study, the results of which are of great importance to current and future research, both on Lewis and other potential WEC array sites.

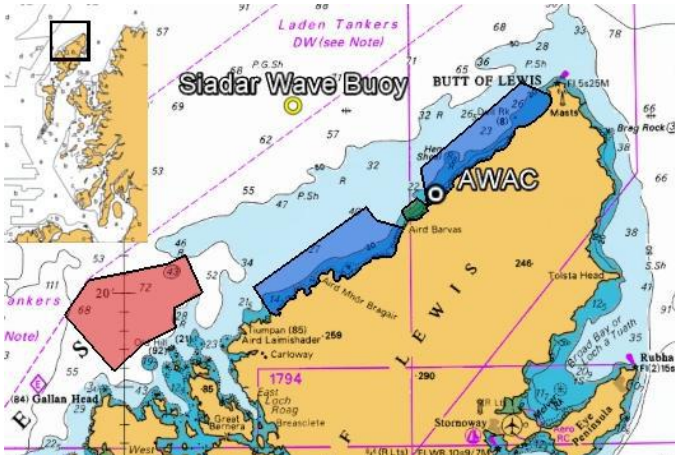

Fig. 1 WEC development sites (West to East: Pelamis Wave Power, Aquamarine Power 1, Voith Hydro Wavegen, and Aquamarine Power 2) and wave data sensors locations.

This study uses Mike 21 SW (Spectral Wave) model produced by DHI (Danish Hydraulic Institute) [7] to simulate the transformation of waves in the nearshore region. Existing wave resource maps and climate data for the area are inadequate for detailed deployment planning, consisting of national maps with low resolution only [8, 9]. These, however, show the highest wave resource of the UK offshore off the Outer Hebrides. While these maps show a general distribution of wave energy, their low resolution and lack of addition information makes them unsuitable for assessing an area for a WEC development.

Over recent years the planned proposals for large scale arrays and the legal obligation to perform EIA has lead to several detailed studies predicting wave-array interactions. One such study uses a SWAN based model to simulate the shoreline change as a result of the installation of a wave farm [10]. This model was driven by frequency spectra generated from a JONSWAP spectrum. The WEC array was treated as a single permeable block and the simulation repeated for several transmission coefficients. The results show a reduction in the downstream wave height dependant on the transmission coefficient, with a larger energy transmission showing a smaller change in the shoreline wave height.

Venugopal and Smith [11] shows the wave–array interactions and the effects of a varying array layout using DHI Mike 21 SW to model the existing wave resource for Orkney Islands before applying the data to Mike 21 BW (Boussinesq Wave) model to simulate the presence of WEC arrays. The arrays are considered as porous structures with known wave energy absorption and the simulation was run for various porosities and layouts. This study shows both the up and downstream wave-device interactions, where wave device reflections can be seen. The results demonstrate that spatial distribution in wave height depends on array layout, and confirm that the change in wave height reduces as porosity is increased and more energy is transmitted.

The previous studies [10, 11] both show a general method of representing WEC arrays as large blocks with frequency independent energy absorptions. More recent research looking at an array of horizontal overtopping devices uses scaled prototype models in a wave tank to obtain a device energy transmission coefficient, which is then applied within a SWAN based model [12]. The model was driven using locational wave climate parameters after a JONSWAP spectrum was applied. The transmission coefficients were then applied to each individual device. A revised version of [10] applies a PTF (Power Transfer Function) based on a damped linear oscillator [13] following previous research from [14]. The PTF is a basic representation of a frequency specific absorption that removes a given amount of energy depending on the device characteristics based on frequency absorption widths. Additional changes see the break-up of the solid array structure into smaller sub-sections. The results of [12, 13] provide the most up to date method of simulating device arrays and show the downstream spatial distribution of the change in resource. However both studies neglect the change in resource from reflective effects and device directionality.

Additional work simulating downstream wake effects of multiple Wave Dragon devices demonstrates the use of the mild slope equations for simulation of large devices [14]. While [14] focuses on sea state and array lay out the purpose of this study demonstrates new methods of simulating devices within existing commercially used software.

The present study uses Mike 21 SW as it has been shown that the software provides a good application for modelling wave propagation in the nearshore region. Mike 21 SW simulates the build-up and transformation of wind and swell waves in the offshore and nearshore environments. This study applies the fully spectral formulation, based on the wave action conservation equation, to simulate the propagation of directional frequency spectra. This allows the model to account for bathymetric refraction and shoaling, wave induced currents, and tidal variations, while wind forcing, nonlinear wave interactions, white capping, bottom friction and depth induced breaking are included as source terms. Diffraction within the model uses a phase-decoupled refraction diffraction approximation; this is based on the mild slope formulation for diffraction and refraction. When a time varying quasi-stationary model is considered the inclusion of diffraction may prevent time step convergence. To prevent this, the software allows the diffraction term to be either smoothed or modelled using a predefined value irrespective of the incident wave climate. By using a cell-centred finite–volume technique the model applies an unstructured mesh grid to propagate the wave action through the model domain using phase averaged equations. Further details on the SW model can be found in the user manual [7]. The application the Mike 21 SW software to simulate the effects of operational WECs are assessed. These results are then applied to bathymetry from the west coast of Lewis, where the effects of a large nearshore WEC array will be presented.

II. MODELLING HYPOTHETICAL WECS

A. Device type and Mike 21 SW

With the large scale proposed developments for the north-west coast of Lewis this study focuses on a large scale

nearshore wave surge oscillator farm. This array is located in the proposed development area for Aquamarine Power [16] where Hebridean Marine Energy Futures has deployed an Acoustic Wave and Current profiler (AWAC). The notional devices are located in the very nearshore waters that follow the 10 m depth contour. As an array of this scale does not currently exist, the changes to the surrounding wave climate are simulated in MIKE 21 SW. Also as the SW model has no specific facility for simulating WECs, this study explores three possible methods of removing energy from the model domain as described below.

Technique -1 WEC as a Source Term: This method uses a spectral wave based tool that applies a source term to a location to simulate the presence of a structure. The source term approach removes energy using a decay term. For energy density E(σ, θ), group wave speed c_g, mesh element area *A* and reflection coefficient c, the source term, *s* is given by

$$s = -\frac{c}{A} c_g E(\sigma, \theta). \quad (1)$$

The size and shape of the structure can be altered to suit a specific device and this study used the default circular pier with a diameter of 20m.

Technique -2 WEC as an Artificial Island: This method of applying a WEC in Mike 21 SW employs a user defined polygon structure. The location, size and shape of the structure are included when the mesh is created. As this study is focusing on an array of nearshore wave surge oscillators dimensions of the structure are 20m x 3m. Polygon structures within Mike 21 SW are interpreted as islands and therefore allow a 0% energy transmission.

Technique -3 WEC as a Reactive Polygon: This method is similar to the artificial island polygon but the up- and downstream device boundaries conditions are modified to produce driving boundaries, where a given wave spectrum maybe emitted. The absorbed spectra are transformed according to the directional frequency relation and reemitted downstream, while the upstream boundary comprises device reflections. The reactive polygons structures used within this study have device dimensions of 20m x 3m.

B. Directional Absorption

When the wave-device interactions for the Reactive Polygon boundaries are considered the energy propagation up and downstream can be effectively controlled. As most wave surge oscillators are directional, only a certain proportion of the directional wave spectra can be absorbed. A formula for the directional absorption coefficient was outlined in [17] and is shown as

$$k_\theta = 0.8 + 0.2(abs(\cos(\theta_{device} - \theta_{wave})))^{0.5} \quad (2)$$

where (θ_{device} - θ_{wave}) is the angle between the device and the incident wave direction. This formula produces a curve with a maximum of 1 for the device when device angle and wave direction are equal. As the incident wave angle diverges from the device angle the absorption coefficient is reduced. This assumption assumes 80% of the wave energy travelling at 90° to the device is absorbed. As this is not the case for a wave surge oscillator this formulation was modified to

$$k_\theta = \left[\mathbb{R}\sqrt{\cos(\theta_{device} - \theta_{wave})}\right]^{2n} \quad (3)$$

where *n* is the absorption width and $\mathbb{R}$ implies taking the real part of the square root (thus ensuring that no energy is absorbed above 90°). If this equation is plotted the effects of *n* can be seen (shown in Fig. 2). As *n* increases the curve becomes narrower but the peak remains at 1. This provides a uni-lateral directional abortion coefficient, where energy is only absorbed when it propagates one direction across the device. This expression shows that as a device gets more directionally sensitive the amount of total absorbed energy reduces as the area under the graph reduces.

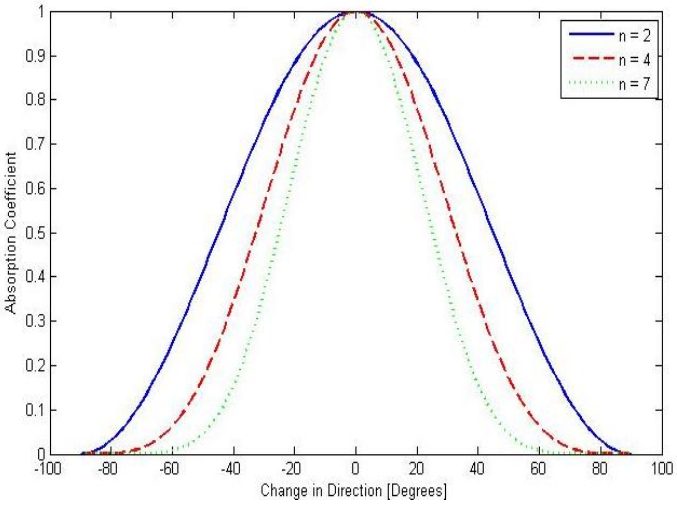

Fig. 2 Modified directional absorption coefficient

When the modified directional absorption is applied to the incident wave spectra at the device location the energy propagating within ±90° will be absorbed dependant on the device relative direction. This study will use an *n* value of 2 as it shows a relatively large absorption width associated with a well designed device.

C. Frequency Absorption

As modern devices are designed to actively resonate with their local wave climate the notion of extracting the same proportion of energy from all frequencies produces an unrealistic Power Transfer Function (PTF). The PTF of devices varies considerably and is dependent on the device and incident wave climate. Currently the energy absorption of a device relative to the incident wave spectra is unavailable. This has led to the development of an approximation that uses a Gaussian curve to simulate energy absorption based on adjustable values from [15] and more recently applied in [13].

This assumption is used to demonstrate the application of PTF and can be shown as

$$PTF(f, f_c, \sigma) = \frac{1}{a\sigma\sqrt{2\pi}} exp\left(-\frac{1}{2}.\frac{(f-f_c)^2}{\sigma^2}\right). \quad (4)$$

Here, f_c is the peak energy frequency, α is an adjustable absorption coefficient and σ is the curve bandwidth. For this

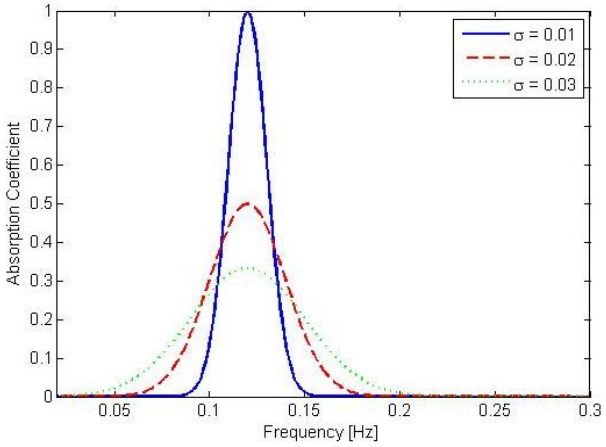

Fig. 3 PTF with varying σ values

purpose α is set to 40 as this produces an absorption coefficient of 1 when the width is set to 0.01. Fig. 3 shows how the level of distribution and peak magnitude are altered as σ is changed. As this is a Gaussian formula the amount of energy absorbed remains constant, allowing similar power rated devices to extract different amount of energy according to device design. This study uses a σ value of 0.01 as this represents a well tuned device with maximum absorption and this provides a realistic high absorption rate.

D. Directional Frequency Absorption

To simulate the device energy absorption from a directional frequency spectrum both the direction and frequency absorption coefficients should be applied. The absorption spectra (S_{abs}) can be shown as

$$S_{abs} = S(1 - (k_\theta . PTF)) \quad (5)$$

where S is the directional frequency spectrum at the WEC location. The absorption spectra consists of the transmitted wave energy as the directional and frequency dependent energies have been removed.

E. Device Reflection

As waves propagate across a device the energy is absorbed from the incident wave spectra. However, a proportion of the remaining energy will also be reflected by the device. The amount of reflected energy depends on multiple factors; this study uses a simplification based on work by [18]. This briefly states that a well tuned wave surge oscillator in a 2-directional field shows an approximate 50% reduction of the incident wave energy, 25% is transmitted in the direction of wave propagation and 25% is reflected. This suggests that approximately 50% is absorbed then 50% of the *remaining* absorption spectra should be reflected from the upstream device boundary. When the incident absorbed and reflected wave energy are shown in the frequency distribution for an example sea state, the magnitude of the reflected and absorbed wave spectra can be seen (see Fig. 4).

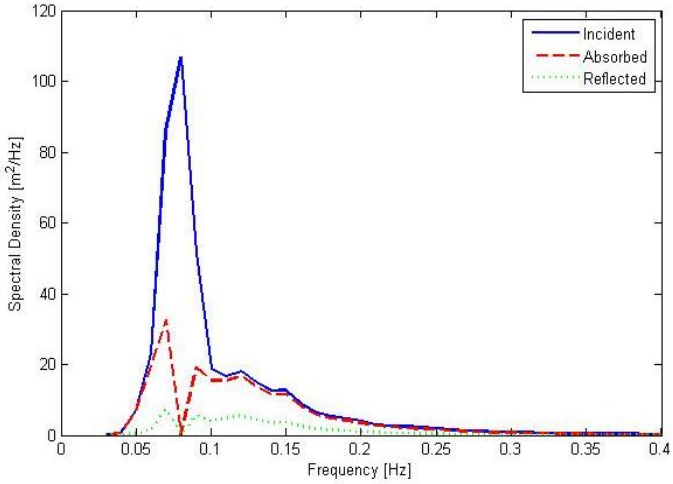

Fig. 4 Wave-device interactions and the frequency energy distribution of an example sea state.

F. Theoretical Single Device Modelling

To determine the best possible method for modelling WEC performance in Mike 21 SW each technique was tested using a theoretical domain. The model domain extends from a 100 m depth with a mesh resolution of approximately 30 m^2 that reduces around the devices to 6 m^2. The simulation was run using a JONSWAP wave spectrum with a peak enhancement factor of (γ) equal to 3.3, resulting in the production of wave parameters H_{m0} = 2 m, T_p = 10 seconds, mean wave direction= 270° and a directional standard deviation = 5°.

G. Theoretical Single Device

Fig. 5 shows the spatial distribution of wave power for each hypothetical WEC. The Source Term modelling technique depicted in (a) shows a wave shadow with a small reduction in wave power behind the WEC device that is extended far downstream. The Artificial Island structure modelling labelled as (b) shows a large reduction in wave power behind the hypothetical device with no alteration to upstream wave field. The Reactive Polygon structure technique (c) shows a similar downstream wave shadow however there is a significant reduction of the absorbed wave energy resulting in a smaller reduction in wave power downstream of the device. The upstream wave field in (c) shows a significant increase in power by reflected waves that reduces as the distance upstream of the device increases.

To better quantify the change in the spatial wave power distribution as a result of varying device modelling techniques several transects are reviewed. In Fig. 6 a device perpendicular transect is considered, that extends from 150m upstream of the device to 750m downstream. The Source

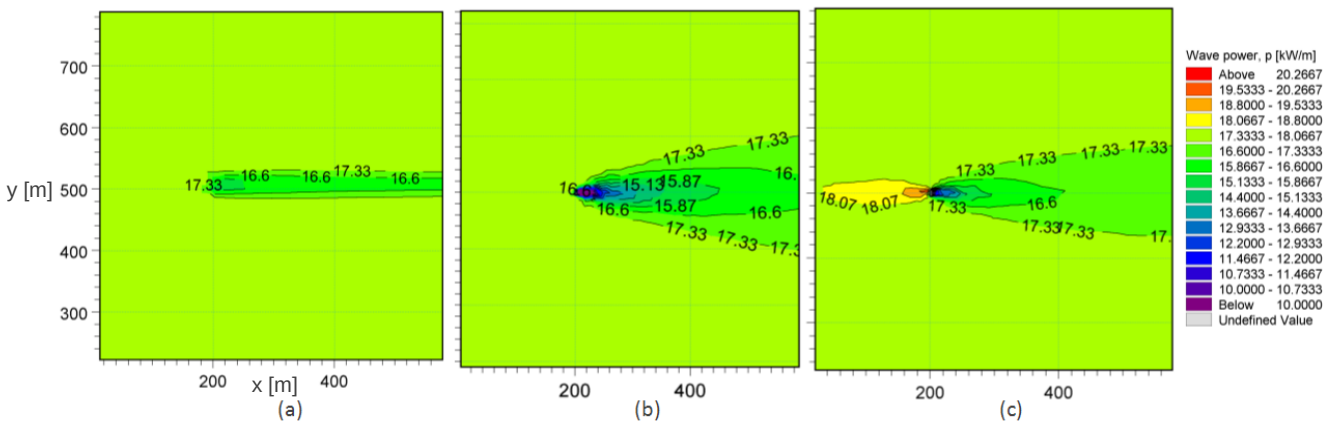

Fig. 5 Wave-device interaction for (a) Technique-1 as Source Term, (b) Technique-2 as Artificial Island (c) Technique-3 as Reactive Polygon structure for the reference sea state in UTM coordinates.

Term technique shows a small peak reduction in wave energy of 2 kW/m a few metres leeward of the device. As the distance increases downstream the wave power shows a small increase with a slow regeneration rate. The Artificial Island technique shows a large peak reduction in wave power of over 14 kW/m leeward of the device. As the distance downstream increases the change in wave power is reduced. The rate of regeneration shows an inverse exponential relationship that becomes less than that of the Source Term method at 450m downstream of the device. The Reactive Polygon technique shows an initial wave power reduction of approximately 5.5 kW/m a few metres behind the device with a similar inverse exponential rate of regeneration as the downstream distance increases. The rate of wave power regeneration of the Reactive Polygon method is almost equal to the incident wave energy at 700m behind the device. The upstream wave interactions show a slight reduction in wave power for the Source Term and the Artificial Island methods. The Reactive Polygon method shows a small increase of 2 kW/m in front of the device that reduces as the distance from the device increases.

When the cross device wave power distribution is plotted at 100m, 300m and 600m behind each device then the evolution of the propagation of the change in wave power can be seen. Fig. 7 shows the wave absorption behind the device where the device is located in the centre of the plot at 500m. The transects were taken 100m, 300m and 600m behind the device, and the results show as the distance increases downstream the change in wave power is reduced. The 100m transect shows the Artificial Island method having the maximum absorption

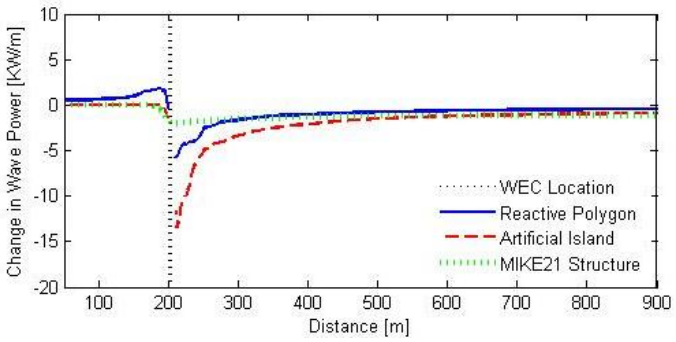

Fig. 6 Change in wave power along the perpendicular transect where y = 500 for each method of modelling a device presented in Fig.5.

of 3.5 kW/m, the Reactive Polygon and the Source Term methods shows a significantly smaller reduction of 2kW/m. For the closest transect all experimental techniques show a narrow absorption bandwidth. With increasing distance downstream, the magnitude of the change in power decreases. 600m behind the device the Artificial Island and the Reactive Polygon methods show a small reduction in wave power when compared to the incident wave power. The Source Term method shows a small reduction as the distance increases from 100m to 600m, this results in the eventual overtaking of the Source Term method by the Artificial Island. Analysis of the spread of the absorption bandwidth shows that the spread increases for the Artificial Island and the Reactive Polygon devices as distance increases. For the Source Term device there is little alteration from the 100m to the 600m transect. Only the Reactive Polygon device shows upstream wave-

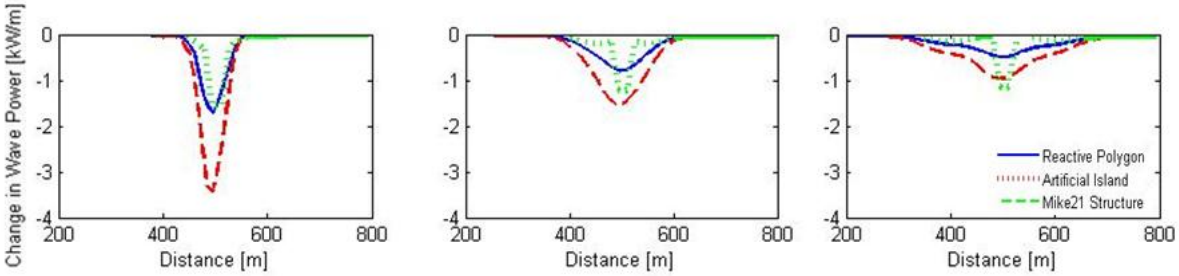

Fig. 7 Change in downstream wave power for device parallel transect downstream of a single device where (left) x = 300m (middle) x = 500m and (right) x = 700m behind the device. Corresponding to 100m, 300m and 500m behind the device.

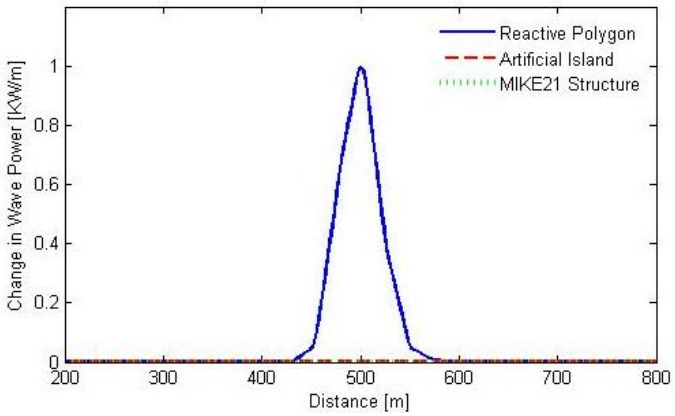

Fig. 8 Change in wave power from a device parallel transect across the y-axis.

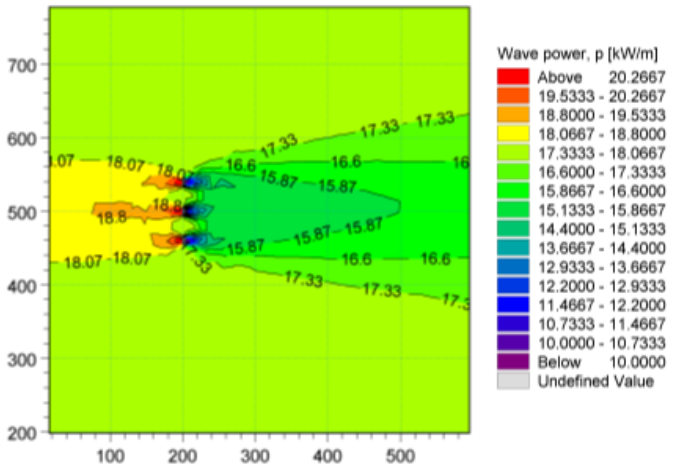

Fig. 9 Wave power distribution around multiple Reactive Polygon devices for the reference sea state.

device interactions. When a device parallel transect is taken 50m upstream of the device the change in wave power from reflective processes can be seen in Fig. 8. The Reactive Polygon device shows an increase in wave power of 1kW/m, whereas the other method of simulating devices shows no alteration in the upstream wave power.

When the downstream wave shadow transects of each hypothetical device are compared with existing literature, the profile shape of the parallel transect of the Artificial Island and Reactive Polygon devices show similarities to that of the work from [12]. However as the diffraction smoothing was not calibrated this comparison is somewhat limited. This may result in the propagation of the wave shadow that only provides an insight into the reduction of wave power behind a device and may not provide realistic solution. As the proposed WEC array is located nearshore, the observed large rate of diffraction shown in this study becomes less significant as the distance to the shore is limited.

The energy transmission coefficient was calculated for each absorption technique. The results show a similar pattern to the wave power transects where techniques 1, 2 and 3 have an energy transmission coefficient of 0.88, 0.0 and 0.50 respectively. This indicates that immediately behind the device the Source Term allows the majority of the wave energy to pass, the Artificial Island allows no energy to propagate across the device and the Reactive Polygon allows half the energy to pass though a device. While techniques 1 and 2 do not account for wave device reflections the Reactive polygon technique has a reflective coefficient of 10.60%. For the purpose of this study the energy transmission coefficient its self is less of a lesser significance as the value of the coefficient is dependent on the incident wave directional standard deviation and the directional frequency absorption parameters applied to the Reactive Polygon.

The single device interactions show that while the Source Term technique is quick to apply within the SW model, further application of the structure is limited due to the limited control over energy transmission. The Artificial Island technique provides a representation of a solid structure with 100% wave power absorption. The shape of the structure can be varied but the inability to select absorption below 100% is a severe limitation. The Reactive Polygon technique allows the use of a more realistic energy transmission where wave absorption is dependent on the incident direction frequency spectra. In addition the upstream boundary of the device allows the propagation of a reflected wave that is dependent on the device absorption. The adaptability of the Reactive Polygon method provides the most realistic device simulation for modelling the potential impacts of an array in this study. The following section will briefly review the effects of multiple Reactive Polygon structures in close proximity in a theoretical domain.

H. Theoretical Array Modelling

For a multiple device test domain, extra polygon structures were added to the north and south of the previous single device mesh. In total, three devices were simulated, allowing for downstream wake interaction without incurring additional complexities. This simulation uses identical model parameters as in the single device tests with the same reference sea state. Fig. 9 shows the spatial wave-device interaction for 3 hypothetical devices. The results show a large downstream reduction in waver power behind each device. As the downstream distance increases the individual effects of each

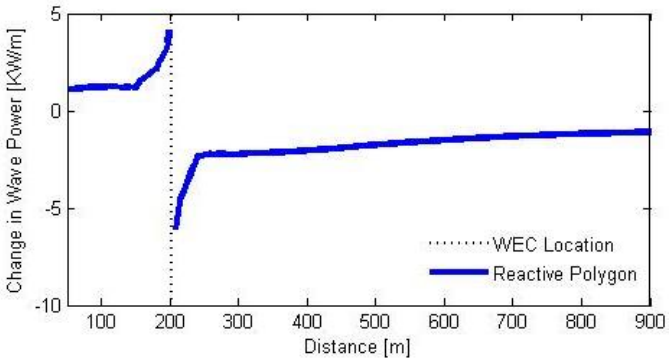

Fig.10 Change in wave power along a device perpendicular transect that bisects the central WEC and spanning the x-axis.

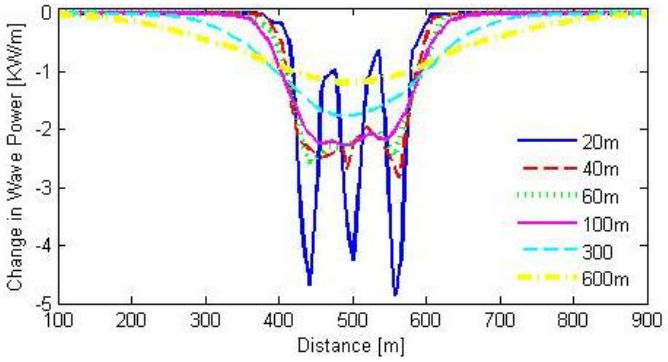

Fig. 11 Change in wave power in lee of the device array plotted in distance across the y axis.

device lessen and merge into a general reduction in wave power. The upstream results show a similar pattern, where individual device reflections propagate and decay into a general increase in wave power as the distance increases. When the change in wave power is considered as device parallel transect for the central device in the array, Fig. 10 shows the downstream wave climate with a greater reduction in wave power. The rate of wave power regeneration shows a significant change approximately 40 m behind the device. The upstream wave climate shows an increase in wave power that diminishes as the distance upstream increases. The maximum increase and decrease in the observed wave power for the multiple device test shows a larger reduction than experienced for a single Reactive Polygon WEC. This indicates the presence of cumulative device effects even at close proximities to the individual devices. When the device perpendicular transects are considered for 20m, 40m , 60m, 100m, 300m, 600m behind the array the evolution of the absorbed wave is shown in Fig. 11. The 20m transect shows 3 clear peak reductions at 440m, 500m and 560m, indicating the presence of the individual devices. As the distance behind the device increases the definition of these peaks are reduced. At 100m downstream there is little sign of individual devices. As the distance increases further, the flat troughed profile broadens resulting in a curved profile with the peak absorption located at the centre of the array. The upstream absorption shows a similar profile for the near device transects. When the 20m upstream transect is plotted (see Fig. 12), the individual device reflections can be seen. As the distance increases, the

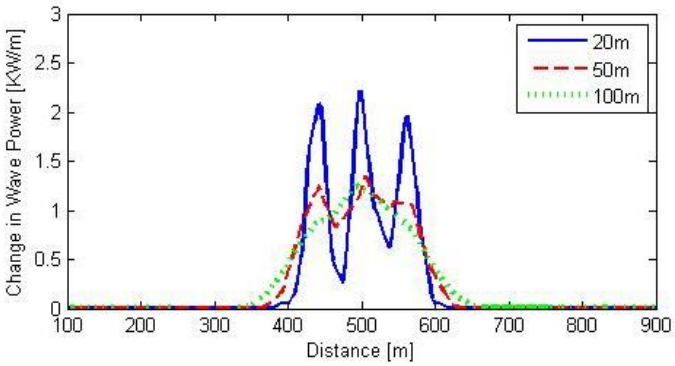

Fig. 12 Upstream change in wave power for a series of transects on the y-axis.

50m transect shows a reduction in the magnitude of increased wave power with less defined peaks for the individual device reflections. At 100m behind the device the reduction in wave power is less severe. The individual device reflections have reduced and merged into a single peak with the largest increase in wave power at the centre of the devices. The results of the theoretical model show a significant increase in the change in wave power around the devices when compared to the individual device results, where the highest change can be seen towards the centre of the array. The larger change in wave power observed in the array test will result in a greater propagation distance of wave-device interactions. This gives a larger wave shadow downstream and a larger reflective effect upstream. By including individual devices the downstream device interactions can be monitored as distance from the devices increases. The results show that the individual device reductions in wave power can be measured up to 300m behind the device. The upstream results show a smaller absolute change in wave power, where the observed individual device reflections do not exceed 100m upstream of the array. This suggests that when modelling the long distance propagation of the wave-array interactions, blocks of WECs may be used. However as the propagation of the wave shadow depends on the incident wave directional spreading, the distances shown within the theoretical tests will vary as the incident wave field changes. As this study considers effects of nearshore WEC arrays, the short distance from device to shoreline will require the use of individual devices to be included within the model.

III. Application to WEC Array

A. Model Setup

The method shown to simulate hypothetical devices was applied to a simulation containing bathymetry and wave data from the west coast of Lewis. The domain construction used multiple sources of bathymetry data with a varying resolution. For the offshore regions the coarse 30 arc second GEBCO 08 data was used. For large proportions of the nearshore and intermediate water depths the domain was covered by Marine Scotland bathymetry data, the resolution of which was reduced for this study to $20m^2$. For shallow water regions near to the proposed WEC array data provided by Aquamarine Power provides an extremely high resolution data, however this data was also reduced to a $20m^2$ resolution for computation requirements. The combined data was used to create two meshes. The first was a simple mesh with no WEC devices. The second mesh was based on the first mesh with 30 Reactive Polygon structures positioned at the south end of the Aquamarine Power 2 site with a reduction in mesh element size surrounding the hypothetical devices .

The driving boundary data was taken from directional wave measurements from a Datawell Waverider MkIII buoy positioned on the domain's north-western boundary. This data was converted into representative directional frequency spectra using a Gaussian directional distribution at a 30minute time step. The data used in this study covers a one year period from December 2011 to December 2012 and was simulated within the model at an hourly time step. The change in water

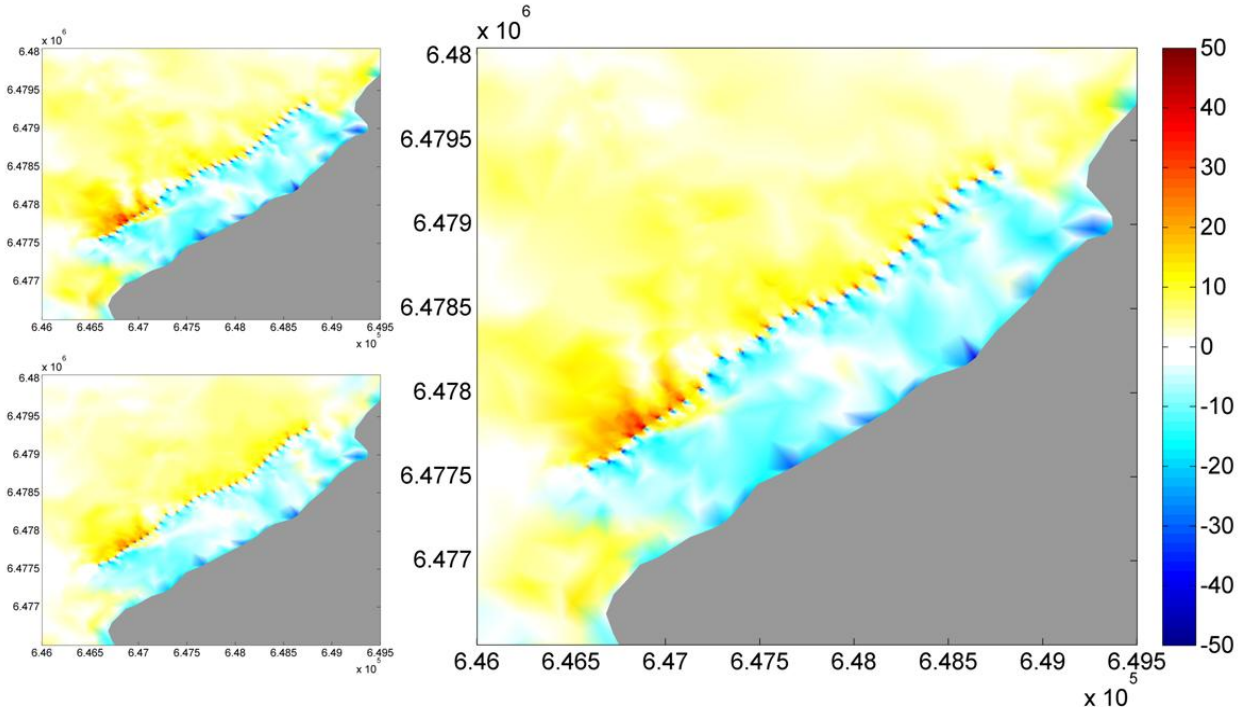

Fig. 13 Percentage change in wave power behind multiple Reactive Polygon structures in UTM-29 coordinates. Top left: winter average, bottom right: summer average and right: yearly average.

level from tidal constituents was included by applying a varying water level across the domain at a 30 minute temporal resolution. The tidal variation time series was generated with DHI's global tidal model for the location of the array. This data was validated using measured data from the AWAC in a previous study [19]. All additional model parameters remain the same as the previous tests.

B. Pre-device Model Calibration and Validation and Device Setup

The pre-array domain was calibrated by varying white capping, bottom friction and wave breaking parameters within the spectral wave model. The pre-device model was run for a one year period at an hourly time step to ensure a year round accurate simulation. The results of this base model were compared with measured data from the AWAC over the same time period. Further details on the calibration processed are outlined in [19]. The results show the modelled wave climate at the AWAC location have an 87% correlation for the significant wave height and 85% for the average wave period. This provides accurate incident wave spectra for each device location, where the absorption and reflection can be calculated.

The individual device locations are situated along the 10m depth contour with an approximate spacing of 60m between devices. The devices were aligned with the 10m depth contour. The addition of the devices provided more node points during the creation of the mesh, resulting in an increased detail of $20m^2$ around the devices.

C. Results and Discussion

The WEC array domain was run for the same time period as the base model. This study reviews the potential changes in spatial wave power for the winter (Dec 2011 - Jan 2012), summer (Jun 2012 – Jul 2012) and yearly average conditions (Dec 2011 – Nov 2012). To provide a detailed comparison the percentage change for each node is calculated. As the number of mesh nodes between the different domains varies, the base model data was interpolated to match the WEC mesh.

Fig. 13 shows the percentage change in the wave power around the devices for each representative spectrum. The location of each device is indicated by a large reduction in power leeward of the device accompanied by a large increase of power in front of the device as seen in the theoretical tests. As there is a large variation in seasonal wave spectra to allow comparison the percentage change in wave power is considered. The distribution of the change in wave power shows the southernmost devices within the array causing a larger impact on the existing wave climate. Further

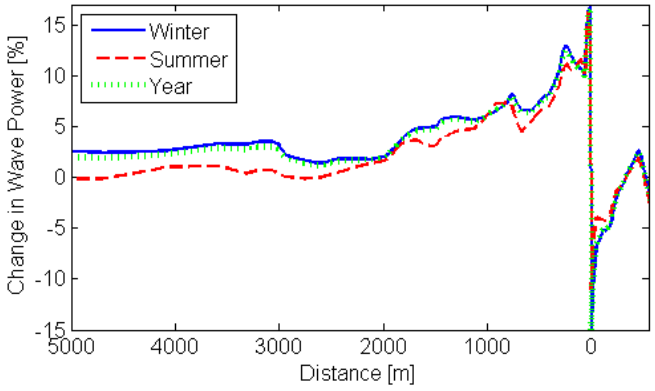

Fig. 14 Change in wave power along the central device perpendicular transect for each seasonal average.

observations show groups of reduced wave power located at the southern and northern end behind the array. The winter average shows a high level of reduced wave power downstream of the devices with a high increase in upstream wave power. The summer results show a lower change in the percentage wave power behind the devices, with a significant change to the very nearshore location. The annual average shows a similar distribution of the change in wave power in lee of array compared to the winter period, however large areas of significant changes in wave power up and downstream of the array are present. Fig. 14 shows a perpendicular transect that bisects the central device. The results show a large reduction in wave power behind all devices with the largest reduction of -15% for the winter and full year averages. The summer seasonal average produces peak values for the change in wave power of -11%. As the distance downstream increases the change wave power reduces and retunes to the pre-device level at approximately 320m behind the device, this value continues increasing and peaks at 420m behind the device with an increase of 2.5 for the winter and yearly results and 1.8 for the summer average. As the distance further increases a second reduction in wave power occurs. This second reduction in wave power occurs in very shallow water, as Mike 21 SW model may not provide accurate convergence for regions of very shallow and/or complex areas these results may be unreliable and should be ignored. The upstream results show a peak change in wave power of above 15% for all representative sea sates. As the distance upstream increases the change in wave power shows a slow decay that propagates beyond 3km. This shows while the reflection contains a small proportion of the incident wave energy the combined upstream propagation causes a significant change to the surrounding wave climate. A downstream transect was taken parallel to, and approximately 350m behind, the central device, extending beyond the width of the array (see Fig. 15). The results show no sign of individual device absorption at the location of the transect. The distribution in the change in power shows the cumulative effects of the wave shadow for all time averaged results. The winter and year averaged results show two regions with increased reductions in wave power. These regions have a peak reduction of 8% and 9.5%. The summer results show a

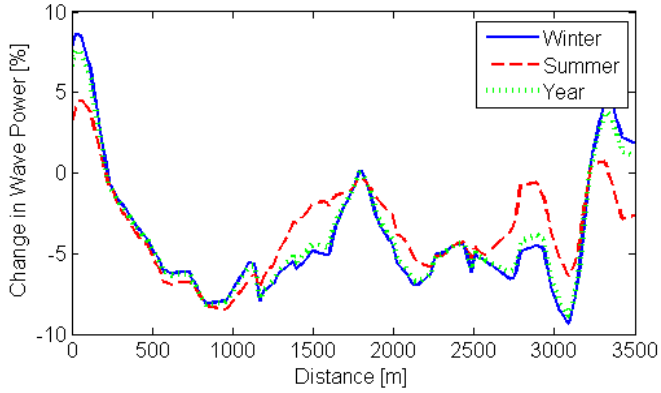

Fig. 15 Change in wave power 300m behind the array for a device parallel transect.

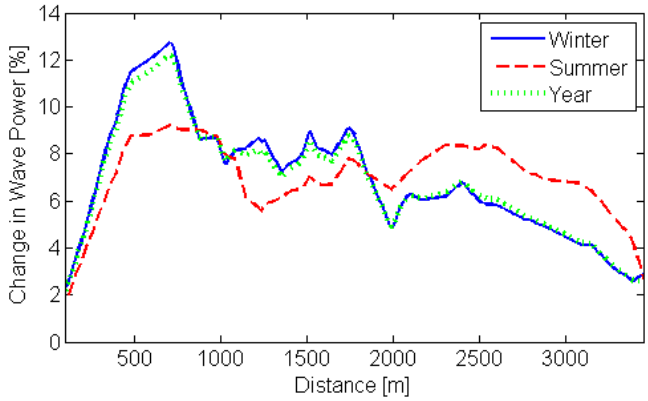

Fig. 16 Change in wave power 300m in front the array for a device parallel transect.

similar variation as the winter and yearly average, however, the central reduction in wave power is much broader with the northern end of the array showing a reduction in variation for the most part. As the transect extends beyond the area directly behind the array the results show an increase in wave power either side of the array for the winter and year averaged results. These results show that the more energetic winter wave conditions cause a larger change in wave power. A further transect is taken approximately 300m upstream of the central array device, and the results are shown in Fig. 16. All results show an increase in wave power, with the largest increase located at the southern end of the array with an increase in power of 12.7% for the winter and year results. For all test conditions the change in wave power at the end of the array tails off. The summer results show a more even distribution of increased power across the upstream transect when compared with the winter and year averaged results. At the northern end of the array a large difference between the winter, annual and summer results can be seen. This difference is likely to be caused by a significant change in the incident wave climate. The winter and year results show a very similar distribution, however the summer average has a general lower magnitude of percentage change. This observed alteration in the distribution of the percentage change may be caused from a seasonal directionally varying wave climate. This change in incident wave climate will cause a significant difference for the absorption and therefore reflective spectra for each device.

The application of the Reactive Polygon technique to the regional bathymetry around the north-west coast of Lewis shows potential for significant nearshore changes to the wave resource. The spatial results show a varying absorption of individual WEC devices that resulting in a cumulative reduction in wave power behind the array. This method also includes the upstream wave-device interaction that shows a large increase in the upstream wave power. By using transects to review the data it can be seen that the incident wave spectrum plays a significant role when assessing the effects of an array on the surrounding wave climate. While seasonal average provides a good approximation to the spatial change in power they exclude the temporal variation containing the extreme results. These excluded periods may contain data important to environmental impacts.

IV. Conclusion

In assessing the potential impacts of WEC on the surrounding wave climate a highly detailed method of simulating a nearshore WEC array has been demonstrated. The theoretical experimentation outlines three possible techniques for modelling WECs and reviews their performance in single and multiple device configurations. Among the three techniques chosen for WEC modelling, the Reactive Polygon technique was found to be the most realistic method., and hence this method was applied to north coast of Lewis at the location of a planned multi-megawatt WEC development. While the methods shown in this study uses hypothetical device characteristics, the flexibility of these technique allows its application to suit a range of WEC technologies and locations.

The result show the more complex Reactive Polygon method provides the most realistic simulation as it accounts for device specific directional and frequency factors. When the Reactive Polygon technique was applied to the average winter, summer and one year wave conditions for a proposed WEC array consisting of 30 devices, the changes to the wave climate were observed. The results indicate the average yearly reduction in nearshore wave power is 5%, this value increases to a peak value of 9.5% during the winter average at the nearshore location. The upstream results show an increase in percentage change, where the yearly average shows an increase of approximately 7.5% that extends as high as 12.7% at the southernmost end of the array. The results show that the spatial distribution in wave power is strongly based on the device-incident wave climate and the device absorption parameters. This study shows that the inclusion of the reflective wave field provides important information not only for environmental effect but for regions with multiple WEC developments, where reflective waves may alter the existing resource at neighbouring development size. While the methods shown within this study were applied to the current environment conditions, the absorption values used were not intended to represent a particular device performance, and power takeoff behaviour can vary significantly between device types and models.

The further development of the processes to quantify the change in wave climate due to WEC arrays has provided a new technique for simulating WECs on a regional scale. While the predicted changes to the surrounding wave climate provide an insight into the potential effects an array may have on this location, further work looks at a temporally varying simulation that includes storm events to determine additional changes in wave power in specific conditions. Additional work should focus on including a realistic diffraction term that allows for a more appropriate regeneration of wave energy behind a device within Mike 21 SW.

Acknowledgment

The authors wish to acknowledge the funding received from the European Regional Development Fund and the primarily SFC funded Hebridean Marine Energy Futures Project. Furthermore the author is grateful for the data and support from the Hebridean Marine Energy Futures project partners Aquamarine Power and Lews Castle College.

References

[1] Scottish Government, *2020 Route Map for Renewable Energy in Scotland*, 2011.

[2] E.ON Climate &Renewable UK Ltd, *Loch Urr Wind – Environmental Impact Assessment Scoping Report*, 2012.

[3] DP Marine Energy Ltd, *Islay Tidal Energy Project – Environmental Impact Assessment Scoping Report*, 2009.

[4] Aquamarine Power, www.aquamarinepower.com

[5] Pelamis Wave Power, www.pelamiswave.com

[6] Voith Hydro Wavegen, www.wavegen.co.uk

[7] Danish Hydraulic Institute, *MIKE 21 Spectral Waves FM – Short Description*, Hørsholm, Denmark. 2011.

[8] The Crown Estate, *UK Wave and Tidal Key Resource Areas Project Summary Report*, [Online]. Available www.thecrownestate.co.uk/ media/355255/uk-wave-and-tidal-key-resource-areas-project.pdf. (2012).

[9] Carbon Trust, *UK Wave Energy Resource*, [Online]. Available www.carbontrust.com/media/202649/ctc816-uk-wave-energy-resource.pdf. 2012.

[10] D.L. Millar, H.C.M. Smith, D.E. Reeve, *Modelling analysis of the sensitivity of shoreline change to a wave farm*, Ocean Engineering, vol 34, pp.884-901, 2006.

[11] V. Venugopal, G.H. Smith, Wave Climate Investigation for an Array of Wave Power Devices" Proc. 7th European Wave and Tidal Energy Conference, Porto, Portugal. 2007.

[12] R. Carballo, G. Iglesias, *Wave farm impact based on realistic wave-WEC interactions*, Energy [Online] Available http://dx.doi.org/10. 1016/j.energy.2012.12.040

[13] H.C.M. Smith, C. Pearce, D.L. Millar, *Further analysis of change in nearshore wave climate due to an offshore wave farm: An enhanced case study for the Wave Hub site.* Renewable Energy, vol 40 , pp.51-64, 2012.

[14] C. Beels, P. Troch, K.D. Visch, J.P. Kofoed, G.D Backer, *Application of the Time-Dependent Mild-Slope Equations for the Simulation of Wake Effects in the Lee of a Farm of Wave Dragon Wave Energy Converters*, Renewable Energy, vol 35, issue 8, pp 1644-2661, 2010.

[15] G.H Smith , V.Venugopal, J. Fasham, *Wave spectral bandwidth as a measure of available wave power*, Proc. 25th international Conference of Offshore Mechanics an Arctic Engineering. 2006.

[16] Aquamarine Power, Lewis Wave Power Limited, *40MW Oyster Wave Array North West Coast, Isle of Lewis – Environmental Statement*, 2012.

[17] T. Boehme, J. Taylor, R. Wallace, J. Bialek, *Matching Renewable Energy Generation with Demand*,[Online]. Available http://www. scotland. gov.uk/ Publications/2006/04/24110728/10, 2006

[18] A. Henry, K. Doherty, L. Cameron, T. Whitter, R. Doherty, *Advances in the Design of the Oyster Wave Energy Converter* Proc. The Royal Institution of Naval architecture, Marine and Offshore Renewable Energy Conference, London, UK, 2010.

[19] C. Greenwood, V. Venugopal, D. Christie, J. Morrison, A. Vögler, *Wave Modelling for Potential Wave Energy Sites around the Outer Hebrides*, Proc. 32th International Conference on Ocean, Offshore and Arctic Engineering, 2013.